Quantum Monte Carlo Calculations with Chiral Effective Field Theory Interactions

A. Gezerlis,[1,2,*] I. Tews,[1,2] E. Epelbaum,[3] S. Gandolfi,[4] K. Hebeler,[5] A. Nogga,[6] and A. Schwenk[2,1]

[1]*Institut für Kernphysik, Technische Universität Darmstadt, 64289 Darmstadt, Germany*
[2]*ExtreMe Matter Institute EMMI, GSI Helmholtzzentrum für Schwerionenforschung GmbH, 64291 Darmstadt, Germany*
[3]*Institut für Theoretische Physik II, Ruhr-Universität Bochum, 44780 Bochum, Germany*
[4]*Theoretical Division, Los Alamos National Laboratory, Los Alamos, New Mexico 87545, USA*
[5]*Department of Physics, The Ohio State University, Columbus, Ohio 43210, USA*
[6]*Institut für Kernphysik, Institute for Advanced Simulation and Jülich Center for Hadron Physics,
Forschungszentrum Jülich, 52425 Jülich, Germany*

We present the first quantum Monte Carlo (QMC) calculations with chiral effective field theory (EFT) interactions. To achieve this, we remove all sources of nonlocality, which hamper the inclusion in QMC calculations, in nuclear forces to next-to-next-to-leading order. We perform auxiliary-field diffusion Monte Carlo (AFDMC) calculations for the neutron matter energy up to saturation density based on local leading-order, next-to-leading order, and next-to-next-to-leading order nucleon-nucleon interactions. Our results exhibit a systematic order-by-order convergence in chiral EFT and provide nonperturbative benchmarks with theoretical uncertainties. For the softer interactions, perturbative calculations are in excellent agreement with the AFDMC results. This work paves the way for QMC calculations with systematic chiral EFT interactions for nuclei and nuclear matter, for testing the perturbativeness of different orders, and allows for matching to lattice QCD results by varying the pion mass.

Chiral effective field theory (EFT) has revolutionized the theory of nuclear forces by providing a systematic expansion for strong interactions at low energies based on the symmetries of quantum chromodynamics [1–3]. Chiral interactions have been successfully employed in calculations of the structure and reactions of light nuclei [4–7], medium-mass nuclei [8–14], and nucleonic matter [15–21]. While continuum quantum Monte Carlo (QMC) methods are very precise for strongly interacting systems [22,23], including neutron matter [24–28], and have provided pioneering calculations of light nuclei [29,30], QMC methods have not been used with chiral EFT interactions due to nonlocalities in their present implementation in momentum space. In this Letter, we take up this challenge and combine the accuracy of QMC methods with the systematic chiral EFT expansion. As an application, we study the neutron matter equation of state up to nuclear densities. Neutron matter constitutes an exciting system because of its connections to ultracold atoms and its importance for the physics of neutron-rich nuclei, neutron stars, and supernovae. Our work opens up nonperturbative benchmarks of nuclear matter for astrophysics, including studies of hyperons, based on chiral EFT, as well as the matching to the underlying theory of QCD through lattice simulations.

First, we explain how to remove all sources of nonlocality in chiral EFT interactions to next-to-next-to-leading order (N²LO) and present local nucleon-nucleon (*NN*) interactions at leading order (LO), next-to-leading order (NLO), and N²LO based on Ref. [31]. We use the developed chiral

potentials for the first time in QMC calculations to study neutron matter order by order including theoretical uncertainties. The nonperturbative QMC results provide many-body benchmarks and enable us to test perturbative calculations for the same interactions.

The difficulty of handling nonlocal interactions in QMC methods (see also Ref. [32]) results from how interactions enter. Continuum QMC methods are based on a path-integral evaluation using propagators of the form

$$G(\mathbf{R}, \mathbf{R}'; \delta\tau) = \langle \mathbf{R} | e^{-\delta\tau \hat{O}} | \mathbf{R}' \rangle, \qquad (1)$$

where $\mathbf{R} = (\mathbf{r}_1, \mathbf{r}_2, \ldots, \mathbf{r}_N)$ is the configuration vector of all N particles (plus spins and other quantum numbers), $\delta\tau$ is a step in the imaginary-time evolution, and the operator $\hat{O}$ takes into account the kinetic energy and the interaction part of the Hamiltonian. The implementation of continuum QMC methods relies on being able to separate all momentum dependences as a quadratic $\sum_{i=1}^{N} \mathbf{p}_i^2$ term, which is the case for local interactions, but not for general momentum-dependent, nonlocal interactions (spin-orbit interactions, linear in momentum, are manageable). In the local case, the propagator for the momentum-dependent part is a Gaussian integral that can be evaluated analytically, and the effects of interactions concern only the positions of the particles.

Chiral EFT interactions are based on a momentum expansion and are therefore naturally formulated in momentum space [1,2]. To regularize interactions at high momenta, one employs regulator functions, usually of the form $f(p) = e^{-(p/\Lambda)^{2n}}$ and $f(p')$, where $\mathbf{p} = (\mathbf{p}_1 - \mathbf{p}_2)/2$

and $\mathbf{p}' = (\mathbf{p}'_1 - \mathbf{p}'_2)/2$ are the incoming and outgoing relative momenta, respectively. Upon Fourier transformation, this leads to nonlocal interactions $V(\mathbf{r}, \mathbf{r}')$ already due to the choice of regulator functions. The other sources of nonlocality in chiral EFT are due to contact interactions that depend on the momentum transfer in the exchange channel $\mathbf{k} = (\mathbf{p}' + \mathbf{p})/2$ and to $\mathbf{k}$-dependent parts in pion-exchange contributions beyond N²LO. In contrast, dependences on the momentum transfer $\mathbf{q} = \mathbf{p}' - \mathbf{p}$ are local, and lead to nonlocalities only because of the regulator functions used.

To avoid regulator-generated nonlocalities for the long-range pion-exchange parts of chiral EFT interactions, we use the local coordinate-space expressions for the LO one-pion-exchange and NLO and N²LO two-pion-exchange interactions [33,34] and regulate them directly in coordinate space using the function $f_{\text{long}}(r) = 1 - e^{-(r/R_0)^4}$, which smoothly cuts off interactions at short distances $r < R_0$ while leaving the long-range parts unchanged. So, R_0 takes over the role of the cutoff Λ in momentum space. To regularize the pion loop integrals of the two-pion-exchange contributions, we use a spectral-function regularization [34] with cutoff $\tilde{\Lambda} = 800$ MeV. For the N²LO two-pion-exchange interactions we take the low-energy constants $c_1 = -0.81$ GeV^{-1}, $c_3 = -3.4$ GeV^{-1}, and $c_4 = 3.4$ GeV^{-1} as in the momentum-space N²LO potential of Ref. [35].

To remove the $\mathbf{k}$-dependent contact interactions to N²LO, we make use of the freedom to choose a basis of short-range operators in chiral EFT interactions (similar to Fierz ambiguities). At LO, one usually considers the two momentum-independent contact interactions $C_S + C_T \boldsymbol{\sigma}_1 \cdot \boldsymbol{\sigma}_2$. However, it is equivalent to choose any two of the four operators $\mathbb{1}$, $\boldsymbol{\sigma}_1 \cdot \boldsymbol{\sigma}_2$, $\boldsymbol{\tau}_1 \cdot \boldsymbol{\tau}_2$, and $\boldsymbol{\sigma}_1 \cdot \boldsymbol{\sigma}_2 \boldsymbol{\tau}_1 \cdot \boldsymbol{\tau}_2$, with spin and isospin operators $\boldsymbol{\sigma}_i$, $\boldsymbol{\tau}_i$, because there are only two S-wave channels due to the Pauli principle. It is a convention in present chiral EFT interactions to neglect the isospin dependence, which is then generated from the exchange terms.

We use this freedom to keep at NLO (order Q^2) an isospin-dependent q^2 contact interaction and an isospin-dependent $(\boldsymbol{\sigma}_1 \cdot \mathbf{q})(\boldsymbol{\sigma}_2 \cdot \mathbf{q})$ tensor part in favor of a nonlocal k^2 contact interaction and a nonlocal $(\boldsymbol{\sigma}_1 \cdot \mathbf{k})(\boldsymbol{\sigma}_2 \cdot \mathbf{k})$ tensor part. This leads to the following seven linearly independent contact interactions at NLO that are local,

$$V_{\text{short}}^{\text{NLO}} = C_1 q^2 + C_2 q^2 \boldsymbol{\tau}_1 \cdot \boldsymbol{\tau}_2 + (C_3 q^2 + C_4 q^2 \boldsymbol{\tau}_1 \cdot \boldsymbol{\tau}_2) \boldsymbol{\sigma}_1 \cdot \boldsymbol{\sigma}_2$$
$$+ i\frac{C_5}{2}(\boldsymbol{\sigma}_1 + \boldsymbol{\sigma}_2) \cdot \mathbf{q} \times \mathbf{k} + C_6(\boldsymbol{\sigma}_1 \cdot \mathbf{q})(\boldsymbol{\sigma}_2 \cdot \mathbf{q})$$
$$+ C_7(\boldsymbol{\sigma}_1 \cdot \mathbf{q})(\boldsymbol{\sigma}_2 \cdot \mathbf{q}) \boldsymbol{\tau}_1 \cdot \boldsymbol{\tau}_2, \qquad (2)$$

where the only $\mathbf{k}$-dependent contact interaction (C_5) is a spin-orbit potential. Because at NLO the only two possible momentum operators allowed by symmetries are q^2 and k^2 (or equivalently $p^2 + p'^2$ and $\mathbf{p} \cdot \mathbf{p}'$), and similarly for the

tensor parts, it is thus possible to remove all sources of nonlocality in chiral EFT to N²LO. In addition, the leading $3N$ forces at N²LO can be constructed as local interactions [36,37], but we will first focus on QMC calculations with chiral NN interactions. The next-higher order (Q^4) NN contact interactions enter at N³LO, and there are too many possible operators involving $\mathbf{k}$, so that they cannot be traded for isospin dependence completely. Therefore, chiral EFT interactions will contain nonlocal terms at N³LO, but one may expect that these high-order nonlocal parts can be treated perturbatively.

Upon Fourier transformation, these LO and NLO contact interactions lead to local smeared-out delta functions $\delta_{R_0}(\mathbf{r})$ and their derivatives when a local regulator $f_{\text{local}}(q^2)$ is used. We implicitly define the local regulator by taking $\delta_{R_0}(\mathbf{r}) \sim e^{-(r/R_0)^4}$ with an exponential regulator (with the same scale R_0) similarly as for the long-range parts. We thus have for the LO contact interactions in coordinate space

$$\int \frac{d\mathbf{q}}{(2\pi)^3} C_{S,T} f_{\text{local}}(q^2) e^{i\mathbf{q} \cdot \mathbf{r}} = C_{S,T} \frac{e^{-(r/R_0)^4}}{\pi \Gamma(\frac{3}{4}) R_0^3}, \qquad (3)$$

where the denominator is determined by normalization. The analogous local expressions involving the NLO contact interactions are obtained by replacing $C_{S,T}$ with the seven different operators of Eq. (2). Finally, for the range of the scale R_0 we consider $R_0 = 0.8$–1.2 fm corresponding to typical momentum cutoffs $\Lambda \sim 600$–400 MeV in chiral EFT interactions. This follows Weinberg's power counting with typical cutoffs of order the breakdown scale ~ 500 MeV [1,38]. The same local rearrangement can be applied to modified power counting [39], to pionless EFT [40], to power counting that includes k_F as an explicit scale [41], and when making use of off-shell ambiguities [42].

The low-energy couplings $C_{S,T}$ at LO plus C_{1-7} at NLO and N²LO are fit in Ref. [31] for different R_0 to the NN phase shifts of the Nijmegen partial-wave analysis [43] at laboratory energies $E_{\text{lab}} = 1, 5, 10, 25, 50,$ and 100 MeV. The reproduction of the isospin $T = 1$ S and P waves is shown order by order in Fig. 1, where the bands are obtained by varying R_0 between 0.8–1.2 fm and provide a measure of the theoretical uncertainty. For the $R_0 = 1.2$ fm N²LO NN potential, we list the low-energy couplings at LO, NLO, and N²LO in Table I. At N²LO, an isospin-symmetry-breaking contact interaction (C_{nn} for neutrons) is added in the spin $S = 0$ channel (to $C_S - 3C_T$), which is fit to a scattering length of -18.8 fm. As shown in Fig. 1, the comparison with NN phase shifts is very good for $E_{\text{lab}} \lesssim 150$ MeV. This is similar for higher partial waves and isospin $T = 0$ channels, which will be reported in a later paper that will also study improved fits. In cases where there are deviations for higher energies (such as in the $^3P_2$ channel of Fig. 1), the width of the band signals significant theoretical uncertainties due to the chiral EFT truncation at N²LO. The NLO and N²LO bands nicely overlap (as shown for the cases in Fig. 1), or are very
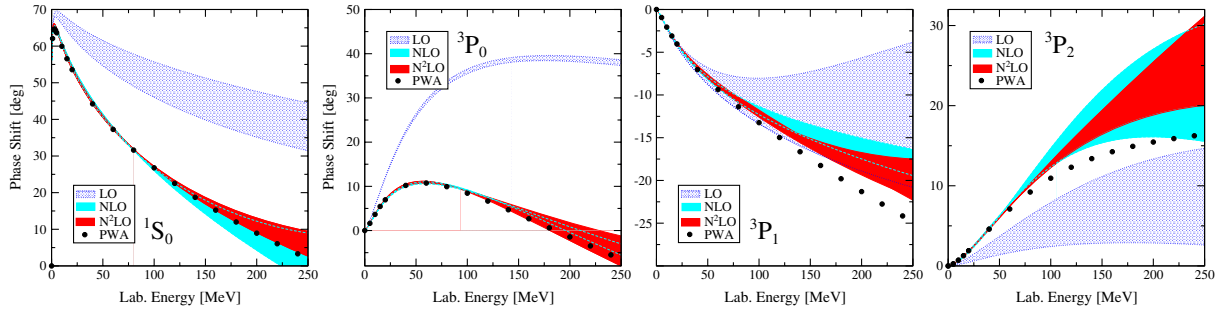
FIG. 1 (color online).   Neutron-proton phase shifts as a function of laboratory energy $E_{\text{lab}} = 2p^2/m$ in the $^1S_0$, $^3P_0$, $^3P_1$, and $^3P_2$ partial waves (from left to right) in comparison to the Nijmegen partial-wave analysis (PWA) [43]. The LO, NLO, and N^{2}LO bands are obtained by varying R_0 between 0.8–1.2 fm (with a spectral-function cutoff $\tilde{\Lambda} = 800$ MeV).

close, but it is also apparent that the N^{2}LO bands are of a similar size as at NLO. This is because the width of the bands at both NLO and N^{2}LO shows effects of the neglected order-Q^4 contact interactions.

Finally, we emphasize that the newly introduced local chiral EFT potentials include the same physics as the momentum-space versions. This is especially clear when antisymmetrizing. Besides the new idea of removing the k^2 terms, there are no conceptual differences between the two ways of regularizing (see also the early work [44]).

We then apply the developed local LO, NLO, and N^{2}LO chiral EFT interactions in systematic QMC calculations for the first time. Since nuclear forces contain quadratic spin, isospin, and tensor operators (of the form $\boldsymbol{\sigma}_i^\alpha A_{ij}^{\alpha\beta} \boldsymbol{\sigma}_j^\beta$), the many-body wave function cannot be expressed as a product of single-particle spin-isospin states. All possible spin-isospin nucleon-pair states need to be explicitly accounted for, leading to an exponential increase in the number of possible states. As a result, Green's function Monte Carlo (GFMC) calculations are presently limited to 12 nucleons and 16 neutrons [30]. In this Letter, we would like to simulate $O(100)$ neutrons to access the thermodynamic limit. We therefore turn to the auxiliary-field diffusion Monte Carlo (AFDMC) method [45], which is capable of efficiently handling spin-dependent Hamiltonians.

TABLE I.   Short-range couplings for $R_0 = 1.2$ fm at LO, NLO, and N^{2}LO (with a spectral-function cutoff $\tilde{\Lambda} = 800$ MeV) [31]. The couplings C_{1-7} are given in fm^4 while the rest are in fm^2.

	LO	NLO	N^{2}LO
C_S	-1.83406	-0.64687	1.09225
C_T	0.15766	0.58128	0.24388
C_1		0.18389	-0.13784
C_2		0.15591	0.07001
C_3		-0.13768	-0.13017
C_4		0.02811	0.02089
C_5		-1.99301	-1.82601
C_6		0.26774	0.18700
C_7		-0.25784	-0.24740
C_{nn}			0.05009

Schematically, AFDMC rewrites the Green's function by applying a Hubbard-Stratonovich transformation using auxiliary fields to change the quadratic spin-isospin operator dependences to linear. As a result, when applied to a wave function that is a product of single-particle spin-isospin states, the new propagator independently rotates the spin of every single nucleon. Using this approach, central and tensor interactions can be fully included in an AFDMC stochastic simulation. For the case of neutrons, it has also been possible to include fully in AFDMC spin-orbit interactions and three-body forces [46,47].

We first studied finite-size effects and the dependence on the Jastrow correlations in the trial Jastrow-Slater wave function (in continuum QMC calculations there are no discretization effects). The dependence on particle number was found to be nearly identical to that of the noninteracting Fermi system, consistent with results using phenomenological NN potentials [47]. Therefore, we performed calculations for an optimal number of 66 particles, while also including contributions from the 26 cells neighboring the primary simulation box. We also compared the neutron matter energy at a density 0.1 fm^{-3} starting from no to full Jastrow correlations based on the same R_0 local chiral NN interactions versus Jastrow correlations of the hard Argonne v_8' potential, as a first step in probing the general dependence on the Jastrow term. For the softer $R_0 = 1.2$ fm ($R_0 = 0.8$ fm) interactions the changes of the energy per particle are at most 0.1 MeV (0.6 MeV), which corresponds to 1% (5%) changes. This appears to be related to the way the propagator is sampled with tensor and spin-orbit interactions and will be studied in detail in a forthcoming paper. The exact results should be independent of the trial wave function, but we consider Jastrow correlations based on the same R_0 interactions more consistent and use these.

In Fig. 2 we present first AFDMC calculations for the neutron matter energy with chiral EFT NN interactions at LO, NLO, and N^{2}LO. Our results represent nonperturbative energies for neutron matter based on chiral EFT beyond low densities. For neutrons, the AFDMC method has been carefully benchmarked with nuclear GFMC, which can handle beyond-central correlations as well as release the nodal or
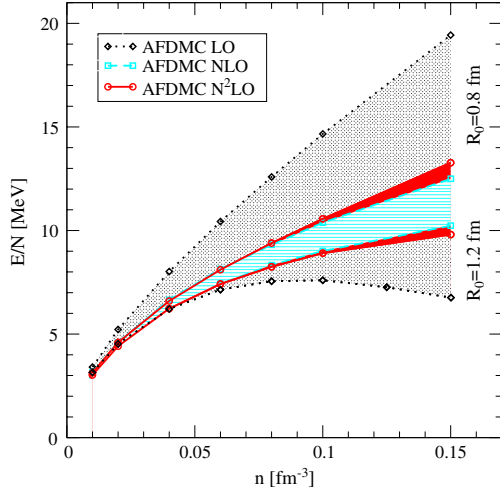
FIG. 2 (color online). Neutron matter energy per particle E/N as a function of density n calculated using AFDMC with chiral EFT NN interactions at LO, NLO, and N^2LO. The statistical errors are smaller than the points shown. The lines give the range of the energy band obtained by varying R_0 between 0.8–1.2 fm (as for the phase shifts in Fig. 1), which provides an estimate of the theoretical uncertainty at each order. The N^2LO band is comparable to the one at NLO due to the large c_i couplings in the N^2LO two-pion exchange.

FIG. 3 (color online). The AFDMC N^2LO band of Fig. 2 in comparison to perturbative calculations of the neutron matter energy using the same local N^2LO NN interactions. The lower (upper) limit of the AFDMC N^2LO band is for $R_0 = 1.2$ fm ($R_0 = 0.8$ fm), corresponding to a momentum cutoff $\Lambda \sim 400$ MeV ($\Lambda \sim 600$ MeV). Perturbative results are shown for Hartree-Fock plus second-order contributions (2nd order) and including third-order particle-particle and hole-hole corrections (3rd order). The bands at 2nd and 3rd order are obtained by using a Hartree-Fock or free single-particle spectrum. For the softer $R_0 = 1.2$ fm interaction (narrow purple bands), the third-order corrections are small and the perturbative third-order energy is in excellent agreement with the AFDMC results, while for the harder $R_0 = 0.8$ fm interaction (light red bands), the convergence is clearly slow. At low densities, we also show the QMC (2010) results of Refs. [28,51].

phase constraint after convergence to the ground state. Both have been found to have minimal effects on the equation of state of neutrons [47–49]. At each order, the full interaction is used both in the propagator and when evaluating observables. The bands in Fig. 2 give the range of the energy obtained by varying R_0 between 0.8–1.2 fm, where the softer $R_0 = 1.2$ fm interactions yield the lower energies. At low densities (low Fermi momenta), as expected the energy is well constrained at LO, with small corrections at NLO due to effective range effects [50,51]. AFDMC enables us to present results up to saturation density (and higher, but we emphasize that the contributions of $3N$ forces will become important for densities $n \gtrsim 0.05$ fm^{-3} [17]). At LO, the energy has a large uncertainty. The overlap of the bands at different orders in Fig. 2 is excellent. In addition, the result that the NLO and N^2LO bands are comparable is expected due to the large c_i entering at N^2LO; this is similar to the phase shift bands in Fig. 1. At the highest density studied, the size of the N^2LO band is approximately 10% of the potential energy, which will be improved by including $3N$ forces [17] and going to higher order [20]. Therefore, our first QMC results for neutron matter exhibit a systematic order-by-order convergence in chiral EFT. Given the small contributions coming from $3N$ forces at intermediate density, as well as the limited size of the systematic error bands there, our results are a nonperturbative benchmark that can lead to further predictions at higher density, when $3N$ forces are consistently included.

Our AFDMC results provide first nonperturbative benchmarks for chiral EFT interactions at nuclear densities. We have performed perturbative calculations
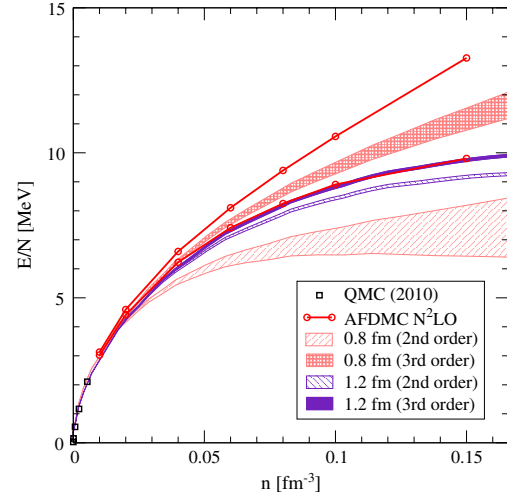
following Refs. [17,18,20] based on the same local N^2LO NN interactions at the Hartree-Fock level plus second-order contributions and including third-order particle-particle and hole-hole corrections. At each order, we give bands obtained by using a Hartree-Fock or free single-particle spectrum. The perturbative energies are compared in Fig. 3 to the AFDMC N^2LO results. For the softer $R_0 = 1.2$ fm ($\Lambda \sim 400$ MeV) interaction, the third-order corrections are small and the perturbative third-order energy is in excellent agreement with the AFDMC results, while for the harder $R_0 = 0.8$ fm ($\Lambda \sim 600$ MeV) interaction, the convergence is clearly slow. This is the first nonperturbative validation for neutron matter of the possible perturbativeness of low-cutoff $\Lambda \sim 400$ MeV interactions [52]. Finally, in the low-density regime, the results in Fig. 3 match the QMC calculations of Refs. [28,51] based on central interactions that reproduce the large neutron-neutron scattering length and the effective range physics.

In summary, we have presented the first QMC calculations with chiral EFT interactions. This was achieved by using a freedom in chiral EFT to remove all sources of nonlocality to N^2LO. We have constructed local LO, NLO,

and N^{2}LO NN interactions, given in operator form times local potentials $V(r)$ in coordinate space. The reproduction of the NN phase shifts is very good compared to the momentum-space N^{2}LO NN potentials of Ref. [35]. Direct application of the local chiral NN interactions in AFDMC sets first nonperturbative benchmarks for the neutron matter equation of state at nuclear densities. Our results show systematic order-by-order convergence with theoretical uncertainties and validate perturbative calculations for the softer local NN interactions. Future AFDMC calculations with local N^{2}LO $3N$ forces will provide *ab initio* constraints for nuclear density functionals and for dense matter in astrophysics. This work paves the way for QMC calculations with systematic chiral EFT interactions for nuclei, neutron drops, and nuclear matter. Regarding nuclear matter, a perturbative approach has been able to predict realistic saturation properties using parameters fit only to few-body systems [18], so future QMC work will be key to validating this and to providing nonperturbative benchmarks. By direct matching to lattice QCD results [53] (for example, for few-neutron systems in a box) also varying the pion mass in chiral EFT, the approach presented here will be able to connect nuclear physics to the underlying theory of QCD.

---

*gezerlis@theorie.ikp.physik.tu-darmstadt.de

[1] E. Epelbaum, H.-W. Hammer, and U.-G. Meißner, Rev. Mod. Phys. **81**, 1773 (2009).
[2] D. R. Entem and R. Machleidt, Phys. Rep. **503**, 1 (2011).
[3] H.-W. Hammer, A. Nogga, and A. Schwenk, Rev. Mod. Phys. **85**, 197 (2013).
[4] N. Kalantar-Nayestanaki, E. Epelbaum, J. G. Messchendorp, and A. Nogga, Rep. Prog. Phys. **75**, 016301 (2012).
[5] B. R. Barrett, P. Navrátil, and J. P. Vary, Prog. Part. Nucl. Phys. **69**, 131 (2013).
[6] R. Roth, J. Langhammer, A. Calci, S. Binder, and P. Navrátil, Phys. Rev. Lett. **107**, 072501 (2011).
[7] E. Epelbaum, H. Krebs, D. Lee, and U.-G. Meißner, Phys. Rev. Lett. **104**, 142501 (2010); **106**, 192501 (2011); E. Epelbaum, H. Krebs, T. A. Lahde, D. Lee, and U.-G. Meißner, Phys. Rev. Lett. **110**, 112502 (2013).
[8] T. Otsuka, T. Suzuki, J. D. Holt, A. Schwenk, and Y. Akaishi, Phys. Rev. Lett. **105**, 032501 (2010).
[9] J. D. Holt, T. Otsuka, A. Schwenk, and T. Suzuki, J. Phys. G **39**, 085111 (2012); J. D. Holt, J. Menéndez, and A. Schwenk, J. Phys. G **40**, 075105 (2013).
[10] G. Hagen, M. Hjorth-Jensen, G. R. Jansen, R. Machleidt, and T. Papenbrock, Phys. Rev. Lett. **108**, 242501 (2012); **109**, 032502 (2012).
[11] R. Roth, S. Binder, K. Vobig, A. Calci, J. Langhammer, and P. Navrátil, Phys. Rev. Lett. **109**, 052501 (2012).
[12] H. Hergert, S. K. Bogner, S. Binder, A. Calci, J. Langhammer, R. Roth, and A. Schwenk, Phys. Rev. C **87**, 034307 (2013).
[13] V. Soma, C. Barbieri, and T. Duguet, Phys. Rev. C **87**, 011303 (2013).
[14] F. Wienholtz *et al.*, Nature (London) **498**, 346 (2013).
[15] N. Kaiser, S. Fritsch, and W. Weise, Nucl. Phys. **A697**, 255 (2002).
[16] E. Epelbaum, H. Krebs, D. Lee, and U.-G. Meißner, Eur. Phys. J. A **40**, 199 (2009).
[17] K. Hebeler and A. Schwenk, Phys. Rev. C **82**, 014314 (2010).
[18] K. Hebeler, S. K. Bogner, R. J. Furnstahl, A. Nogga, and A. Schwenk, Phys. Rev. C **83**, 031301 (2011).
[19] K. Hebeler, J. M. Lattimer, C. J. Pethick, and A. Schwenk, Phys. Rev. Lett. **105**, 161102 (2010).
[20] I. Tews, T. Krüger, K. Hebeler, and A. Schwenk, Phys. Rev. Lett. **110**, 032504 (2013); arXiv:1304.2212.
[21] J. W. Holt, N. Kaiser, and W. Weise, Phys. Rev. C **87**, 014338 (2013).
[22] D. M. Ceperley, Rev. Mod. Phys. **67**, 279 (1995).
[23] J. Carlson, S. Gandolfi, and A. Gezerlis, Prog. Theor. Exp. Phys. (**2012**) 01A209.
[24] A. Gezerlis and J. Carlson, Phys. Rev. C **77**, 032801(R) (2008).
[25] G. Wlazłowski and P. Magierski, Phys. Rev. C **83**, 012801 (2011).
[26] A. Gezerlis, Phys. Rev. C **83**, 065801 (2011).
[27] S. Gandolfi, J. Carlson, and S. Reddy, Phys. Rev. C **85**, 032801(R) (2012).
[28] A. Gezerlis and R. Sharma, Phys. Rev. C **85**, 015806 (2012).
[29] B. S. Pudliner, V. R. Pandharipande, J. Carlson, S. C. Pieper, and R. B. Wiringa, Phys. Rev. C **56**, 1720 (1997).
[30] S. C. Pieper, Riv. Nuovo Cimento **31**, 709 (2008).
[31] M. Freunek, Diploma thesis, Universität Bonn and Forschungszentrum Jülich, 2007.
[32] J. E. Lynn and K. E. Schmidt, Phys. Rev. C **86**, 014324 (2012).
[33] N. Kaiser, R. Brockmann, and W. Weise, Nucl. Phys. **A625**, 758 (1997).
[34] E. Epelbaum, W. Glöckle, and U.-G. Meißner, Eur. Phys. J. A **19**, 125 (2004).
[35] E. Epelbaum, W. Glöckle, and U.-G. Meißner, Nucl. Phys. **A747**, 362 (2005).
[36] P. Navrátil, Few-Body Syst. **41**, 117 (2007).
[37] A. Lovato, O. Benhar, S. Fantoni, and K. E. Schmidt, Phys. Rev. C **85**, 024003 (2012).
[38] G. P. Lepage, arXiv:nucl-th/9706029.
[39] A. Nogga, R. G. E. Timmermans, and U. van Kolck, Phys. Rev. C **72**, 054006 (2005); B. Long and C.-J. Yang, Phys. Rev. C **86**, 024001 (2012), and references therein.

[40] J. Kirscher, H. W. Grießhammer, D. Shukla, and H. M. Hofmann, Eur. Phys. J. A **44**, 239 (2010).

[41] A. Lacour, J. A. Oller, and U.-G. Meißner, Ann. Phys. (Amsterdam) **326**, 241 (2011).

[42] E. Oset, A. Martinez Torres, K. P. Khemchandani, L. Roca, J. Yamagata, Prog. Part. Nucl. Phys. **67**, 455 (2012), and references therein.

[43] V. G. J. Stoks, R. A. M. Klomp, M. C. M. Rentmeester, and J. J. de Swart, Phys. Rev. C **48**, 792 (1993).

[44] C. Ordóñez, L. Ray, and U. van Kolck, Phys. Rev. C **53**, 2086 (1996).

[45] K. E. Schmidt and S. Fantoni, Phys. Lett. B **446**, 99 (1999).

[46] A. Sarsa, S. Fantoni, K. E. Schmidt, and F. Pederiva, Phys. Rev. C **68**, 024308 (2003).

[47] S. Gandolfi, A. Yu. Illarionov, K. E. Schmidt, F. Pederiva, and S. Fantoni, Phys. Rev. C **79**, 054005 (2009).

[48] J. Carlson, J. Morales, Jr., V. R. Pandharipande, and D. G. Ravenhall, Phys. Rev. C **68**, 025802 (2003).

[49] S. Gandolfi, J. Carlson, and S. C. Pieper, Phys. Rev. Lett. **106**, 012501 (2011).

[50] A. Schwenk and C. J. Pethick, Phys. Rev. Lett. **95**, 160401 (2005).

[51] A. Gezerlis and J. Carlson, Phys. Rev. C **81**, 025803 (2010).

[52] S. K. Bogner, R. J. Furnstahl, and A. Schwenk, Prog. Part. Nucl. Phys. **65**, 94 (2010).

[53] S. R. Beane, E. Chang, S. D. Cohen, W. Detmold, H. W. Lin, T. C. Luu, K. Orginos, A. Parreno, M. J. Savage, and A. Walker-Loud, Phys. Rev. D **87**, 034506 (2013).